ELSEVIER

Journal of Alloys and Compounds 275–277 (1998) 318–322

Journal of ALLOYS AND COMPOUNDS

Electronic structures of highly symmetrical compounds of f elements XXXI Simulation of the crystal field splitting pattern of $(THF)_3Li(\mu\text{-}Cl)Nd[N(SiMe_3)_2]_3$

S. Jank, H. Reddmann, H.-D. Amberger*

Institut für Anorganische und Angewandte Chemie der Universität Hamburg, Martin-Luther-King-Platz 6, 20146 Hamburg, Germany

Abstract

The absorption spectra of an unoriented single crystal of the title compound (**1**) have been measured at room and at low temperatures. Assuming a similar sequence of crystal field (CF) levels as for the previously analyzed $Nd[N(SiMe_3)_2]_3$ (**2**) a truncated CF splitting pattern is derived from the spectra obtained. The parameters of an empirical Hamiltonian are fitted to the energies of 71 levels to give an r.m.s. deviation of 24.2 cm^{-1}. The parameters obtained are compared with those of **2** and $Nd[N(SiMe_3)_2]_3(CNC_6H_{11})_2$ (**3**). The observed trends of CF parameters are consistent with the results of simple model calculations in the framework of the angular overlap model. © 1998 Elsevier Science S.A.

Keywords: Neodymium; Trimethylsilylamido ligand; Optical spectra; Crystal field analysis

1. Introduction

The tris(bis(trimethylsilyl)amido)lanthanide(III)) $[Ln(btmsa)_3]$ complexes, which are highly soluble in inert hydrocarbons, are considered as extremely valuable precursors for the syntheses of THF free molecular complexes of the lanthanides [1]. However, adopting the original preparation as suggested by Bradley et al. [2] the powdered precursor $Ln(btmsa)_3$ itself as well as the target complexes exhibited THF containing by-products [3,4]. At first we thought that these impurities were caused by a mono THF adduct of $Ln(btmsa)_3$, but an X-ray analysis of a single crystal (which grew as the least soluble compound from a recrystallisation of crude products of $Nd(btmsa)_3$ (**2**)) exhibited the existence of $(THF)_3Li(\mu\text{-}Cl)Nd(btmsa)3$ (**1**) [5]. Unfortunately, this work paralleled only a previous X-ray analysis of Edelmann et al. [4].

Recently we succeeded in parameterizing the experimentally derived cyrstal field (CF) splitting patterns of base-free [6] and of the bis(cyclohexylisocyanide)adduct of **2**(**3**) [7]. It is the aim of this contribution to derive the (truncated) CF splitting pattern of **1** on the basis of absorption measurements and to subsequently fit the parameters of an empirical Hamiltonian [8,9] to this splitting pattern.

2. Experimental details

By cooling down a nearly saturated solution of crude (unsublimed) **2** in *n*-pentane from boiling to ambient temperature (within 1 h) some big and a number of small crystals were grown. Inspecting these crystals by a polarizing microscope, revealed that most of them showed the expected straight, but some exhibited skew extinction. An X-ray analysis of a small crystal with skew extinction proved the composition $(THF)_3Li(\mu\text{-}Cl)Nd(btmsa)_3$. Details of the sealing procedure of a bigger crystal (6×2×2 mm) with skew extinction as well as details of the absorption measurements are given elsewhere [6]. The actual temperature of the measurements was approximately 50 K. In order to improve the heat transfer we tried also to run absorption spectra of solutions and pellets. However **1** decomposes in solution as well as during the pellet pressing procedure.

*Corresponding author. Fax: +49 40 4123 2893; e-mail: fc3a501@rrz.uni-hamburg.de

0925-8388/98/$19.00
PII: S0925-8388(98)00331-4

3. Results

3.1. Derivation of the CF splitting pattern

Considering only the first coordination sphere, the Nd^{3+} central ion is surrounded by the three N atoms of the btmsa ligands and the Cl^- ion in the shape of a slightly distorted trigonal pyramid (see Fig. 1), thus we assume an effective CF of C_{3v} symmetry.

The principal threefold axes of the eight molecules per unit cell are aligned, therefore linear dichroism measurements of oriented single crystals should be possible, in principle. However, several attempts to record these spectra were not successful – presumably due to orientation problems with the monoclinic crystals.

Because of the missing information of linear dichroism measurements and because of the similarity of the absorption spectra of **1** and **2** (cf. Figs. 2 and 3) we assumed that the sequences of CF levels for **1** and the previously analyzed **2** [6] are essentially equal. On this basis the experimentally derived CF splitting pattern of **1** – as given in Table 1 – was derived.

3.2. Simulation of the experimentally derived CF splitting pattern

In order to limit the number of free ion parameters of the empirical Hamiltonian applied [8,9], β, γ, the T^i, M^k and P^k parameters were fixed at the values used for the analysis of $LaCl_3$:Nd^{3+} [10]. The remaining parameters were allowed to vary. As a starting parameter set we chose the unchanged free ion parameters used in the CF analysis of **2** [6], in the case of the CF parameters, however, we considered the predictions of calculations in the framework of the angular overlap model [11,12], and increased (in the direction of more positive values) the axial parameters B_0^2, B_0^4 and B_0^6 of **2** by 25%, whereas B_6^6 was adopted unchanged. For 71 levels the r.m.s. deviation was 24.2

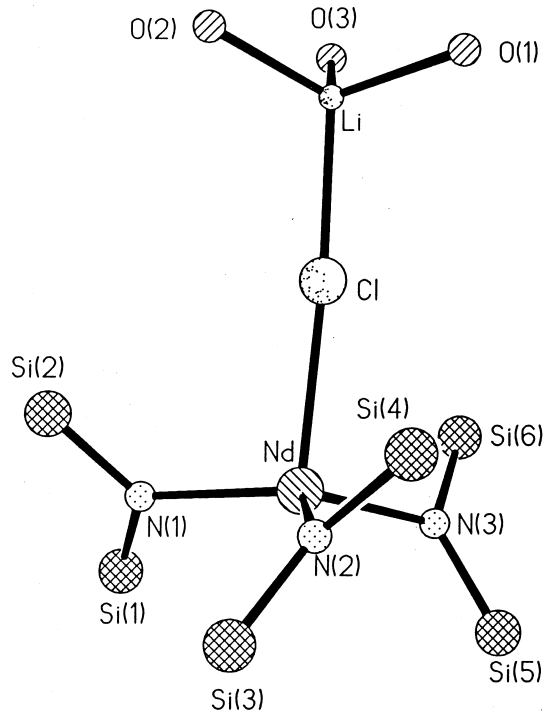

Fig. 1. Molecular structure of $(THF)_3Li(\mu\text{-}Cl)Nd(btmsa)_3$. C and H atoms are not considered.

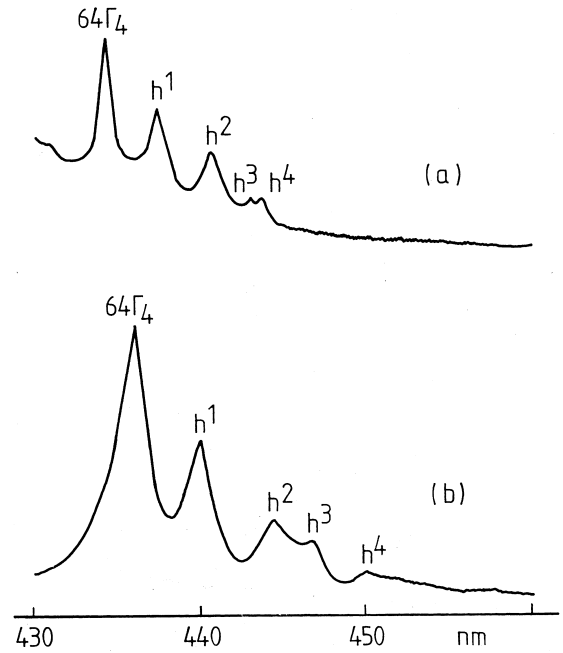

Fig. 2. Comparison of the room temperature absorption spectra of (a) $(THF)_3Li(\mu\text{-}Cl)Nd(btmsa)_3$ and (b) $Nd(btmsa)_3$ in the range 430–460 nm. Signal $64\Gamma_4$ corresponds to the transition originating at the CF ground state and terminating at level $64\Gamma_4$. Hot transitions starting at the first, second, third and fourth excited state and ending at $64\Gamma_4$ are designated as h^1, h^2, h^3 and h^4, respectively.

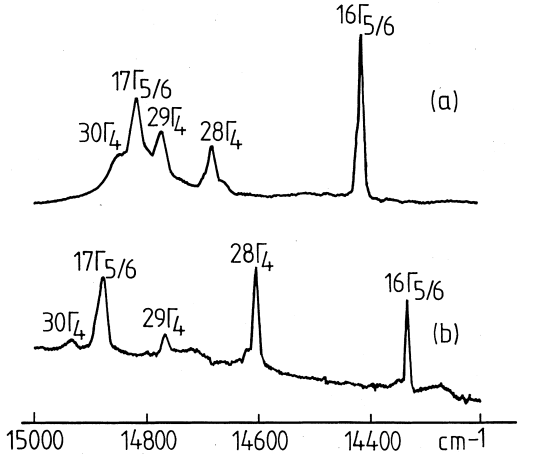

Fig. 3. Comparison of the low temperature absorption spectra of (a) $(THF)_3Li(\mu\text{-}Cl)Nd(btmsa)_3$ and (b) $Nd(btmsa)_3$ in the range 14200–15000 cm^{-1}.

Table 1
Calculated and experimental energy levels for $(THF)_3Li(\mu\text{-}Cl)Nd(btmsa)_3$

SLJ comp.[a]	CF state	$E_{calc.}$ (cm^{-1})	$E_{obs.}$ (cm^{-1})
$^4I_{9/2}$	$1\Gamma_4^b \pm 1/2^c$	0	0
$^4I_{9/2}$	$1\Gamma_{5/6} \pm 3/2$	156	163
$^4I_{9/2}$	$2\Gamma_4 \pm 5/2$	339	324
$^4I_{9/2}$	$3\Gamma_4 \pm 7/2$	455	457
$^4I_{9/2}$	$2\Gamma_{5/6} \pm 9/2$	494	500
$^4I_{11/2}$	$4\Gamma_4 \pm 1/2$	1937	
$^4I_{11/2}$	$3\Gamma_{5/6} \pm 3/2$	2005	
$^4I_{11/2}$	$5\Gamma_4 \pm 5/2$	2115	
$^4I_{11/2}$	$6\Gamma_4 \pm 7/2$	2239	
$^4I_{11/2}$	$4\Gamma_{5/6} \pm 9/2$	2324	
$^4I_{11/2}$	$7\Gamma_4 \pm 11/2$	2363	
$^4I_{13/2}$	$8\Gamma_4 \pm 1/2$	3899	
$^4I_{13/2}$	$5\Gamma_{5/6} \pm 3/2$	3960	
$^4I_{13/2}$	$9\Gamma_4 \pm 5/2$	4062	
$^4I_{13/2}$	$10\Gamma_4 \pm 7/2$	4185	
$^4I_{13/2}$	$6\Gamma_{5/6} \pm 9/2$	4277	
$^4I_{13/2}$	$11\Gamma_4 \pm 11/2$	4329	
$^4I_{13/2}$	$12\Gamma_4 \pm 13/2$	4359	
$^4I_{15/2}$	$13\Gamma_4 \pm 1/2$	5877	
$^4I_{15/2}$	$7\Gamma_{5/6} \pm 3/2$	5958	
$^4I_{15/2}$	$14\Gamma_4 \pm 5/2$	6082	
$^4I_{15/2}$	$15\Gamma_4 \pm 7/2$	6254	
$^4I_{15/2}$	$8\Gamma_{5/6} \pm 9/2$	6359	
$^4I_{15/2}$	$16\Gamma_4 \pm 11/2$	6404	
$^4I_{15/2}$	$17\Gamma_4 \pm 13/2$	6407	
$^4I_{15/2}$	$9\Gamma_{5/6} \pm 15/2$	6439	
$^4F_{3/2}$	$10\Gamma_{5/6} \pm 3/2$	11146	11142
$^4F_{3/2}$	$18\Gamma_4 \pm 1/2$	11523	11566
$^4F_{5/2}$	$19\Gamma_4 \pm 5/2$	12213	12207
$^2H2_{9/2}$	$11\Gamma_{5/6} \pm 9/2$	12354	12408
$^4F_{5/2}$	$12\Gamma_{5/6} \pm 3/2$	12472	12469
$^2H2_{9/2}$	$20\Gamma_4 \pm 1/2$	12534	12547
$^4F_{5/2}$	$21\Gamma_4 \pm 7/2$	12544	12629
$^2H2_{9/2}$	$22\Gamma_4 \pm 5/2$	12643	12668
$^2H2_{9/2}$	$13\Gamma_{5/6} \pm 3/2$	12734	12700
$^2H2_{9/2}$	$23\Gamma_4 \pm 1/2$	12796	12721
$^4F_{7/2}$	$24\Gamma_4 \pm 7/2$	13104	13098
$^4F_{7/2}$	$25\Gamma_4 \pm 5/2$	13364	13362
$^4S_{3/2}$	$14\Gamma_{5/6} \pm 3/2$	13470	13464
$^4S_{3/2}$	$26\Gamma_4 \pm 1/2$	13504	13497
$^4F_{7/2}$	$15\Gamma_{5/6} \pm 3/2$	13546	13539
$^4F_{7/2}$	$27\Gamma_4 \pm 1/2$	13584	13587
$^4F_{9/2}$	$16\Gamma_{5/6} \pm 9/2$	14415	14409
$^4F_{9/2}$	$28\Gamma_4 \pm 7/2$	14653	14680
$^4F_{9/2}$	$29\Gamma_4 \pm 5/2$	14752	14769
$^4I_{9/2}$	$17\Gamma_{5/6} \pm 3/2$	14814	14813
$^4I_{9/2}$	$30\Gamma_4 \pm 1/2$	14855	14848
$^2H2_{11/2}$	$31\Gamma_4 \pm 11/2$	15899	15858
$^2H2_{11/2}$	$18\Gamma_{5/6} \pm 9/2$	15947	15926
$^2H2_{11/2}$	$32\Gamma_4 \pm 7/2$	15975	15964
$^2H2_{11/2}$	$33\Gamma_4 \pm 1/2$	16003	16003
$^2H2_{11/2}$	$19\Gamma_{5/6} \pm 3/2$	16004	16036
$^2H2_{11/2}$	$34\Gamma_4 \pm 5/2$	16017	16059
$^4G_{5/2}$	$35\Gamma_4 \pm 5/2$	16904	16900
$^4G_{5/2}$	$20\Gamma_{5/6} \pm 3/2$	16954	16941
$^4G_{5/2}$	$36\Gamma_4 \pm 5/2$	17085	17024
$^4G_{7/2}$	$37\Gamma_4 \pm 5/2$	17203	17200
$^4G_{5/2}$	$38\Gamma_4 \pm 1/2$	17234	17265
$^4G_{5/2}$	$21\Gamma_{5/6} \pm 3/2$	17238	17265
$^4G_{5/2}$	$39\Gamma_4 \pm 5/2$	17326	17300
$^4G_{7/2}$	$40\Gamma_4 \pm 7/2$	18697	18709
$^2K_{13/2}$	$41\Gamma_4 \pm 5/2$	18804	18801
$^4K_{13/2}$	$22\Gamma_{5/6} \pm 3/2$	18839	18847

Table 1. Continued

SLJ comp.[a]	CF state	$E_{calc.}$ (cm^{-1})	$E_{obs.}$ (cm^{-1})
$^2K_{13/2}$	$42\Gamma_4$ ±1/2	18933	18947
$^4G_{7/2}$	$43\Gamma_4$ ±1/2	19059	19059
$^2K_{13/2}$	$23\Gamma_{5/6}$ ±3/2	19194	19201
$^2K_{13/2}$	$44\Gamma_4$ ±5/2	19329	19342
$^4G_{9/2}$	$24\Gamma_{5/6}$ ±3/2	19374	19387
$^4G_{9/2}$	$45\Gamma_4$ ±5/2	19380	19387
$^4G_{9/2}$	$46\Gamma_4$ ±1/2	19388	19406
$^4G_{9/2}$	$47\Gamma_4$ ±7/2	19448	19448
$^2K_{13/2}$	$25\Gamma_{5/6}$ ±9/2	19459	19470
$^4G_{9/2}$	$48\Gamma_4$ ±7/2	19542	19562
$^2K_{13/2}$	$26\Gamma_{5/6}$ ±9/2	19739	19739
$^2K_{13/2}$	$49\Gamma_4$ ±11/2	19981	19972
$^2K_{13/2}$	$50\Gamma_4$ ±13/2	20182	20169
$^2G1_{9/2}$	$27\Gamma_{5/6}$ ±9/2	20681	20674
$^2K_{15/2}$	$51\Gamma_4$ ±1/2	20765	20790
$^2K_{15/2}$	$28\Gamma_{5/6}$ ±3/2	20809	20807
$^2K_{15/2}$	$52\Gamma_4$ ±5/2	20830	20833
$^2K_{15/2}$	$29\Gamma_{5/6}$ ±7/2	20894	20894
$^2K_{15/2}$	$53\Gamma_4$ ±5/2	20932	
$^2D1_{3/2}$	$54\Gamma_4$ ±1/2	21046	21017
$^2K_{15/2}$	$55\Gamma_4$ ±5/2	21120	21101
$^2G1_{9/2}$	$30\Gamma_{5/6}$ ±9/2	21222	21200
$^4G_{11/2}$	$31\Gamma_{5/6}$ ±9/2	21256	21240
$^4G_{11/2}$	$56\Gamma_4$ ±7/2	21269	21277
$^2K_{15/2}$	$57\Gamma_4$ ±5/2	21310	
$^4G_{11/2}$	$58\Gamma_4$ ±11/2	21343	
$^4G_{11/2}$	$59\Gamma_4$ ±1/2	21492	
$^4G_{11/2}$	$32\Gamma_{5/6}$ ±3/2	21527	21519
$^2K_{15/2}$	$60\Gamma_4$ ±7/2	21545	
$^4G_{11/2}$	$61\Gamma_4$ ±11/2	21569	21561
$^2K_{15/2}$	$33\Gamma_{5/6}$ ±9/2	21634	21640
$^2K_{15/2}$	$62\Gamma_4$ ±11/2	21790	
$^2H_{15/2}$	$63\Gamma_4$ ±13/2	22012	
$^2K_{15/2}$	$34\Gamma_{5/6}$ ±15/2	22240	
$^2P_{1/2}$	$64\Gamma_4$ ±1/2	22999	23020
$^2D1_{5/2}$	$65\Gamma_4$ ±5/2	23297	23240
$^2D1_{5/2}$	$35\Gamma_{5/6}$ ±3/2	23767	23764
$^2D1_{5/2}$	$66\Gamma_4$ ±1/2	24002	24044
$^2P_{3/2}$	$36\Gamma_{5/6}$ ±3/2	25775	25767
$^2P_{3/2}$	$67\Gamma_4$ ±1/2	26080	

[a] Largest eigenvector component.
[b] CF state (C_{3v} symmetry), ordered in ascending energy.
[c] CF state $\pm M_I$ notation.

cm^{-1}. In Table 2 the final values of the free ion and CF parameters are given. For comparison purposes parameters for **2** [6] and **3** [7] are listed too.

4. Discussion

The parameter $(N_v)/\sqrt{(4\pi)} = \sqrt{(\Sigma_{k,q} \quad (1)/(2k+1)(B_q^k)^2)}$ has been proposed as a measure of the strength of the CF [13]. Inserting the CF parameters of **1** into this equation one ends up with a value of 1126 cm^{-1} for $(N_v)/(\sqrt{(4\pi)})$. This value is noticeably lower than that of **2** and greater than that of **3** (cf. Table 2). The considerably decreasing CF strength from **2** to **1** may be explained by an increasing Nd–N distance (2.29 Å in **2** [14], 2.336 Å in **1** [4], but **3** has 2.334 Å, a comparable Nd–N distance as to **1** [7]). The angular overlap model [11,12] predicts increasing B_0^2, B_0^4 and B_0^6 values going from a trigonal planar via a trigonal pyramidal to a trigonal bipyramidal coordination polyhedron, whereas B_6^6 should be essentially constant [15]. The CF parameters of **2** (the structure of which corresponds to an extremely flat trigonal pyramid [14]), **1** and **3** follow this prediction well (see Table 2).

The energy separation of $^2P_{1/2}$ and $^4I_{9/2}$ of Nd^{III} compounds is considered as a measure of covalency [16]. In the case of **1**, **2** and **3** the barycenters of the ground manifold $^4I_{9/2}$ are separated by 22731, 22555 and 22698

Table 2
Parameter values[a] for $(THF)_3Li(\mu\text{-}Cl)Nd(btmsa)_3$, $Nd(btmsa)_3$ and $Nd(btmsa)_3(CNC_6H_{11})_2$ (cm^{-1})

Parameter	$(THF)_3Li(\mu\text{-}Cl)Nd(btmsa)_3$	$Nd(btmsa)_3$[b]	$Nd(btmsa)_3(CNC_6H_{11})_2$[c]
F^2	70205	69980	70219
F^4	52204	51848	52239
F^6	34642	34360	34967
ζ_{4f}	882	882	874
α	21.6	21.8	21.35
β	(−680)	(−680)	(−680)
γ	(1586)	(1586)	(1586)
T^2	(377)	(377)	(377)
T^3	(40)	(40)	(40)
T^4	(63)	(63)	(63)
T^6	(−292)	(−292)	(−292)
T^7	(358)	(358)	(358)
T^8	(354)	(354)	(354)
M^0	(1.97)	(1.97)	(1.97)
M^2	(1.10)	(1.10)	(1.10)
M^4	(0.75)	(0.75)	(0.75)
P^2	(255)	(255)	(255)
P^4	(191)	(191)	(191)
P^6	(127)	(127)	(127)
B_0^2	−2064	−2912	−1712
B_0^4	1073	920	1969
B_0^6	−237	−516	125
B_3^4	1086	–	–
B_3^6	−177	–	–
B_6^6	−333	±331	±390
$Nv/\sqrt{(4\pi)}$	1126	1349	1020

[a] Values in parentheses were not freely varied.
[b] From Ref. [6].
[c] From Ref. [7].

cm^{-1} from $^2P_{1/2}$ [6,7]. Accepting the above mentioned argument, **1** is the least covalent of the three compounds.

Acknowledgements

H.-D.A. wishes to thank the Fonds der Chemischen Industrie for financial support.

References

[1] R. Anwander, Topics Current Chem. 179 (1996) 33.
[2] D.C. Bradley, J.S. Ghotra, F.A. Hart, J. Chem. Soc. Dalton Trans. (1973) 1021.
[3] C. Hagen, H.-D. Amberger, Z. Naturforsch. 48B (1993) 1365.
[4] F.T. Edelmann, A. Steiner, D. Stalke, J.W. Gilje, S. Jagner, M. Hakansson, Polyhedron 13 (1994) 539.
[5] S. Jank, Dissertation, Hamburg, 1998.
[6] H.-D. Amberger, S. Jank, H. Reddmann, N.M. Edelstein, Molec. Phys. 90 (1997) 1013.
[7] H.-D. Amberger, S. Jank, H. Reddmann, J. Hanss, N.M. Edelstein, to be published.
[8] W.T. Carnall, J.V. Beitz, H. Crosswhite, K. Rajnak, J.B. Mann, in: S.P. Sinha (Ed.), Systematics and Properties of the Lanthanides, D. Reidel, Dordrecht, 1982, p. 389.
[9] B.G. Wybourne, Spectroscopic Properties of Rare Earths, Wiley, New York, 1965, p. 166.
[10] W.T. Carnall, H. Crosswhite and H.M. Crosswhite, Energy level structure and transition probabilities in the spectra of the trivalent lanthanides in LaF_3, ANL report, 1997, appendix I, table 1, p. 4, unpublished.
[11] C.K. Jørgensen, R. Pappalardo, H.H. Schmidtke, J. Chem. Phys. 39 (1963) 1422.
[12] C.E. Schäffer, C.K. Jørgensen, Molec. Phys. 9 (1965) 21.
[13] F. Auzel, O.L. Malta, J. Phys. (Paris) 44 (1983) 201.
[14] R.A. Andersen, D.H. Templeton, A. Zalkin, Inorg. Chem. 17 (1978) 2317.
[15] S. Jank, H.-D. Amberger, Acta Phys. Polon. 90 (1996) 21.
[16] E. Antic-Fidancev, M. Lemaitre-Blaise, P. Caro, New J. Chem. (1987) 467.